Preparation and characterization of porous silica spheres by the sol–gel method in the presence of tartaric acid

Hiroyuki Izutsu,[a] Fujio Mizukami,*[b] Padamakumar K. Nair,[b] Yoshimichi Kiyozumi,[b] and Kazuyuki Maeda[b]

[a]*Taki Chemical Co., Ltd. 2, Midorimachi, Befu-cho, Kakogawa, Hyogo 675-01, Japan*

[b]*National Institute of Materials and Chemical Research, 1-1, Higashi, Tsukuba, Ibaraki 305, Japan*

Millimetre-sized mesoporous silica spheres, the sizes of which could be controlled by the mixing speed of the preparation solution, have been prepared directly from the reaction of tetraethoxysilane with tartaric acid in cyclohexanol by the sol–gel process. The silica gel spheres calcined at 400 °C showed specific surface areas of about 850 $m^2 g^{-1}$ and gave sharp pore size distribution curves in the narrow range around 2.3 nm radius. The peak of the pore size distribution curve shifted to smaller values as the calcination temperature increased from 400 to 900 °C. The gel retained a surface area of about 180 $m^2 g^{-1}$ and remained porous even after calcination at 1000 °C. The scanning electron microscope images showed that the spheres are basically composed of closely packed uniform primary particles of diameter *ca.* 20 nm. The high surface area of the spherical gel was considered to be caused by the micropores within the apparent primary particles.

The application of silica spheres is of interest in many fields, including ceramics, catalysis, chromatography, enzyme fixation, *etc*. There are various ways of preparing spherical silicas. The generation of monodisperse, monosized, micrometre spheres of silica from tetraethoxysilane (TEOS) under a highly basic environment was first reported by Stöber *et al*.[1] Later, detailed studies were carried out on the Stöber process.[2–7] The emulsion technique is also a promising method for the synthesis of spherical powders with adjustable particle sizes and defined size distribution. There have been some studies concerning the emulsion technique for the preparation of spherical silica particles;[8–13] however, they mainly concentrated on the size and size distribution of the particles, and in addition the particles studied were below 100 μm in diameter. Only a few results concerning the specific surface area, pore size distribution and gel structure have been reported.

The sol–gel method for preparing metal oxides in powder and film forms has attracted a great deal of attention owing to its characteristic process. Some authors have developed this process by using organic polydentate ligands as modifiers and applied this to the preparation of mixed oxides,[14–16] thermostable alumina[17] and silica.[18] Recently we have observed that a hydroxycarboxylic acid can play a key role in the hydrolysis–condensation processes of tetraethoxysilane during the preparation of high surface area silicas with uniform primary particles,[19,20] and noted that a mixture of tartaric acid, TEOS and a higher alcohol shows hydrophobic properties. In this work, on the basis of our previous results, we prepared silica spheres in the TEOS–tartaric acid–cyclohexanol–water system by a process similar to suspension polymerization. The specific surface area, pore size distribution and pore volume of the spheres, as well as their thermal behaviour, were investigated. In addition, the structure of the spheres was observed by scanning electron microscopy (SEM) and the actual size of the primary particles was checked by transmission electron microscopy (TEM).

Experimental

Preparation of spheres and their size control

Commercial tetraethoxysilane (TEOS), L-tartaric acid (TA) and cyclohexanol were used without purification. TA (0.50 mol) in 0.66 mol of cyclohexanol was mixed with 0.40 mol of TEOS (TA/TEOS = 5/4) in a 1000 ml two-necked flask. The reaction mixture was kept in an oil bath at 80 °C for 2 h with mechanical stirring using a 80 mm mixing blade. A TEOS–TA–cyclohexanol (TTC) mixture became viscous with time owing to the dissolution of TA. Then, 8.0 mol of deionized water (H_2O/TEOS molar ratio = 20) was added to the solution. As the TTC mixture was immiscible with water, when water was added to the solution under stirring, the solution immediately became turbid to give an emulsion. Without stirring, the solution only gave two separated phases. In 60 to 90 min after the addition of water with stirring, the solution became clear and transparent spherical particles came out of the solution spontaneously. The solid spheres were larger than the droplets initially formed in the emulsion; the smaller droplets joined together to form larger ones and they eventually turned into the solid spheres. After 3 h at 80 °C with stirring (250–550 rpm), the spherical particles formed were separated from the solution by filtration, then washed with ethanol and dried at 100 °C in air for 12 h. The spheres after drying were calcined at different temperatures (200, 400, 600, 800, 900, 1000 °C) for 3 h. The spheres were transparent or translucent after drying at 100 °C because organics such as tartaric acid and cyclohexanol were still present. They turned yellow after heating at 400 °C and became white above 600 °C. The yield of silica spheres was 70–80%, which was defined as the ratio of the mass percentage of the particles after heating at 1000 °C to the theoretical SiO_2 amount from starting mixture. After removing the spheres the reaction solution contained a small amount of TEOS and/or its derivatives. Thus, another gel could be obtained by concentrating the filtrate.

The size of the spheres was strongly affected by the stirring rate (Table 1); it decreased as the stirring rate increased.

Table 1 Influence of the stirring speed on the average size of the silica spheres

stirring speed		
rpm	m s^{-1a}	particle size/mm
250	1.05	large masses
300	1.26	0.97[b]
350	1.47	0.95
400	1.68	0.82
450	1.88	0.59
500	2.09	0.35
550	2.30	homogeneous gel

[a]Velocity of the blade edge. [b]Containing irregular particles.

Vigorous stirring resulted in a homogeneous solution and the whole solution finally became a gel. On the other hand, large masses were formed by weak stirring. The sphere sizes which could be obtained reproducibly were in the range 0.3–1.0 mm. Fig. 1 shows the particular spheres formed under the conditions used. However, there were only small differences in specific surface area and pore size distribution between the samples with different sphere sizes. The specific surface areas of the samples calcined at 400 °C were 850–880 m^2 g^{-1}, regardless of their size. Little difference was observed in the most frequent pore size. In this paper, the data for the samples consisting of spheres with diameters *ca.* 1.0 mm are reported.

Characterization

Thermogravimetry and differential thermal analyses (TG–DTA) were carried out on a MAC Science TG–DTA 2100 instrument with a heating rate of 10 °C min^{-1} under a flow of 100 cm^3 min^{-1} dry air. The samples for the TG–DTA measurement were dried at 105 °C for 12 h beforehand. Specific surface area (S_{BET}) was measured by the BET method based on the adsorption of N_2 at 77 K using a Belsorp36 instrument (BEL Japan). Pore size distributions smaller than 100 nm and pore volume (V_P) were evaluated by analysing the N_2 adsorption and desorption isotherms according to the Dollimore–Heal method.[21] External surface areas (S_{ex}, attributable to outer surface) were calculated using a *t*-plot analysis.[22] The distribution of pore diameters larger than 10 nm was determined by mercury porosimetry using a Micromeritics Autopore 9200. SEM and TEM were performed on Hitachi S-800 and JEOL JEM-2010F instruments, respectively.

Results and Discussion

Fig. 2 shows the TG–DTA curves of the uncalcined gel. The mass loss was mainly divided into three temperature regions: below 200 °C, 250–450 °C and above 450 °C. In the DTA curve, the gel showed a large exothermic peak between 250 and 450 °C. Water and ethanol were released at temperatures below 200 °C. On the other hand, the exothermic peak observed at about 350 °C corresponds to the combustion of organic residuals. The mass loss in the range 250–450 °C was almost 20% of the total mass. The gradual loss in mass at higher temperatures could be attributed to the dehydration and condensation of silanols. The results of the TG–DTA studies indicate that organic compounds such as L-tartaric acid or cyclohexanol are likely to remain in the gel.

Fig. 3 shows the SEM images of a cross-section of the sphere calcined at 400 °C. The gel is composed of loose and dense aggregation of small particles. The loose aggregation parts are forming circles (Fig. 3a). The enlargement (Fig. 3b) of the circular section shows that the particles are irregularly condensed and adopt a heterogeneous structure composed of masses of various sizes. However, the greater part of the gel (dense aggregation) is composed of small spherical particles which are about 20 nm in size and packed closely as shown in Fig. 3c. The TEM image (Fig. 4) gives the actual size of the primary particles. Such structural inhomogeneities of silica have also been observed by Scherer.[23] He reported that this characteristic structure results from the phase separation of unhydrolysed TEOS. In Scherer's preparation of silica gel, the amount of water used for hydrolysis was small, less than four mol per mol of TEOS. In the present work, though the amount of water used was large enough, it seems that the hydrolysis was not completed, because the surface of the droplet gels initially, turning into a hard shell which causes slow feeding of water and slow release of organics. Fig. 5 shows the proposed scheme for the reaction route. After the formation of droplets, water dissolves into the TTC droplets through its surface. TEOS in TTC droplets is hydrolysed and the condensation starts from the surface of the droplets. In the opposite direction, ethanol produced by the hydrolysis of TEOS, some TEOS, tartaric acid and cyclohexanol dissolved in ethanol move into the aqueous phase. However, since the reaction system is

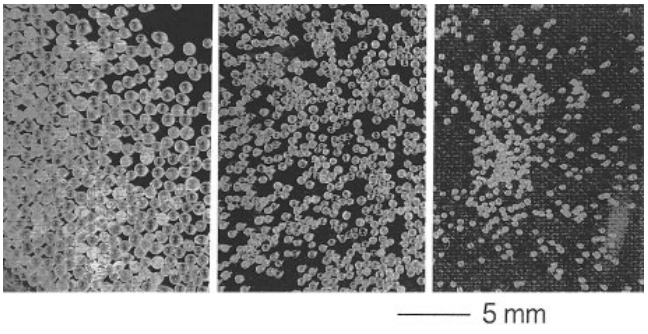

Fig. 1 Photographs of the dried spherical particles with various sizes

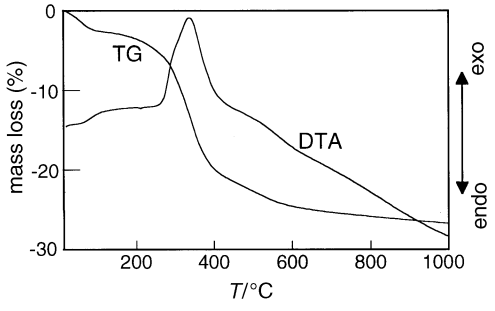

Fig. 2 TG–DTA curves of the uncalcined spherical gel

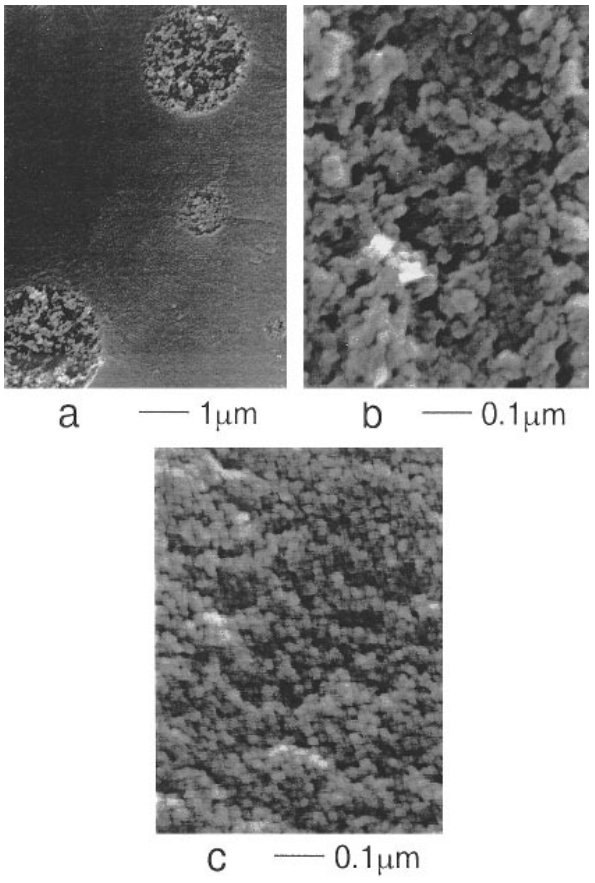

Fig. 3 SEM images of the gel calcined at 400 °C. a, A cross-section of the sphere; b, a magnified image of the circular region; c, a magnified image of the outside of the circular regions.

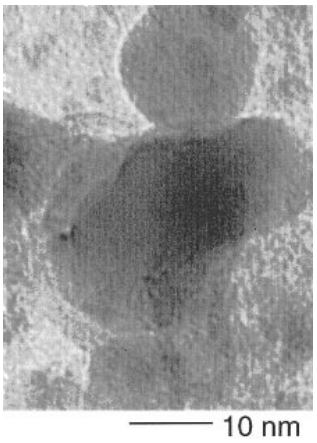

Fig. 4 TEM image of the primary particles constituting the sphere

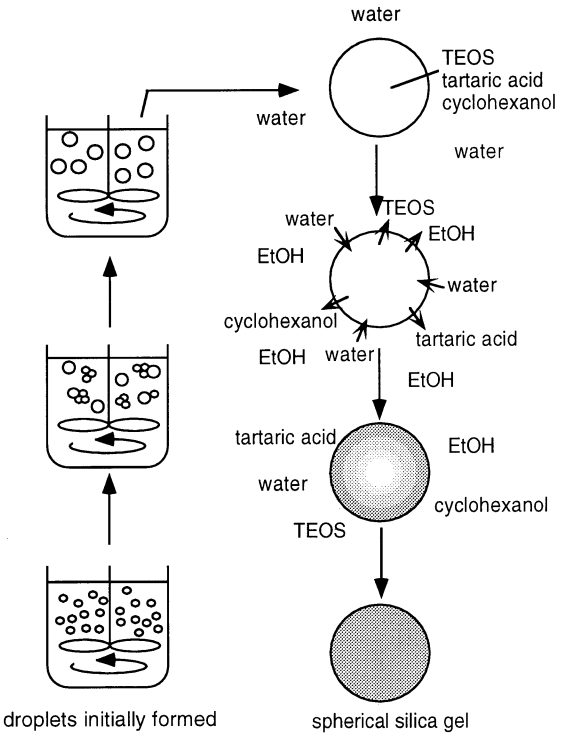

Fig. 5 The proposed scheme for the reaction route

highly acidic, (pH < 1.0, though the measurement of pH in this system is not always accurate), TEOS which exists around the interface and comes into contact with water should be hydrolysed and polycondensed rapidly. Then the gelation and hardening of the droplets proceeds from the surface of the droplets gradually. In fact, the spheres were very soft just after the formation and hardened in an hour as the reaction proceeded. The half-reacted sphere covered with the hard shell still contained a soft core. Although the exact reason why such structural inhomogeneities appear is still unknown, these structural inhomogeneities tend to appear in the case of low hydrolysis water content including the examples in the literature.[23] Thus it could be concluded that the slow and incomplete hydrolysis/condensation reactions inside the droplets by the slow feeding of water caused such phase separation.

From the structure shown in Fig. 3, the sphere is expected to show a certain bimodal pore size distribution curve. Therefore N_2 adsorption/desorption experiments were performed in order to determine the surface areas and pore sizes of the spheres. Fig. 6 shows the nitrogen adsorption and

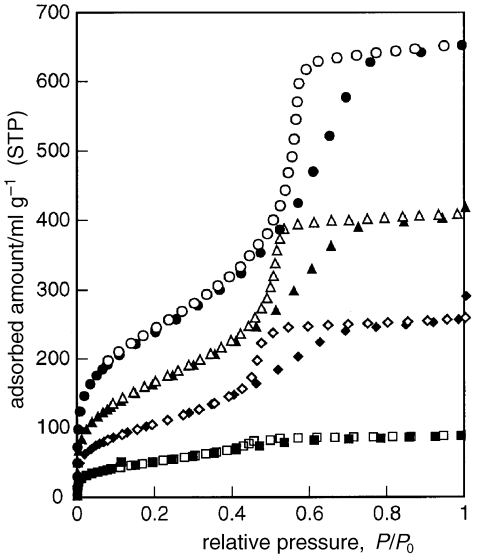

Fig. 6 N_2 adsorption and desorption isotherms of the gels calcined at 400 °C (● ○), 800 °C (▲ △), 900 °C (◆ ◇) and 1000 °C (■ □). Solid symbols, adsorption; open symbols, desorption.

desorption isotherms of the spheres calcined at 400, 800, 900 and 1000 °C. The adsorption isotherms of the spheres calcined below 900 °C were basically of type IV, which is typically observed for mesoporous solids, in the classification by Brunauer, Deming, Deming and Teller (BDDT).[24] However, the spheres also contain micropores as can be seen from the isotherm patterns which show a certain amount of N_2 adsorption in the low pressure region. The hysteresis of the isotherm is classified as type H2 using the IUPAC classification. This H2 type loop is often obtained with corpuscular systems such as silica gel or cracking catalysts, but in these cases the distribution of pore size and shape is not well defined.[25,26] Fundamentally this type of pore may have a structure similar to the H1 type (tubular capillary or narrow-necked ink bottle) in which there is some size distribution in the narrowed part.[26] The pores are considered to be the interstices of the packed spherical particles. Thus, assuming that the pores are ink-bottle shaped, though in practice a series of interconnected pore spaces rather than separate bottles is more likely,[27] the results of N_2 adsorption and desorption measurements were analysed as follows. The adsorption starts inside the wide part of the bottle and then the whole pore is filled up. On the other hand, the desorption occurs through the narrow neck region. Therefore, a pore blocking effect will cause the pore size distribution curve derived from the desorption branch of the isotherm to appear much narrower than that derived from the adsorption branch.[28] This narrowly distributed pore size may be attributable to the size of the neck while the pore size from the adsorption branch gives the size of the body. Actually, as shown in Fig. 7 the pore size distribution estimated from the desorption branch of the isotherm was narrower than that derived from the adsorption branch and the most frequent pore size estimated from the adsorption branch (size of the cavities) was larger. All the samples described below showed the same behaviour. Based on this, the pore size distributions estimated from desorption branches are shown in Fig. 8. The samples calcined at 200 and 400 °C showed sharp pore size distribution curves spread in a narrow range around 2.3 nm radius. The peak of the pore size distribution curve shifted from 2.3 to 1.9 nm as the calcination temperature increased from 400 to 900 °C. Broad pore size distributions around 20 nm radius were also observed for the samples calcined at 200, 400 and 600 °C. These might be attributable to the larger pores (loose aggregation) observed in Fig. 3a. Pores larger

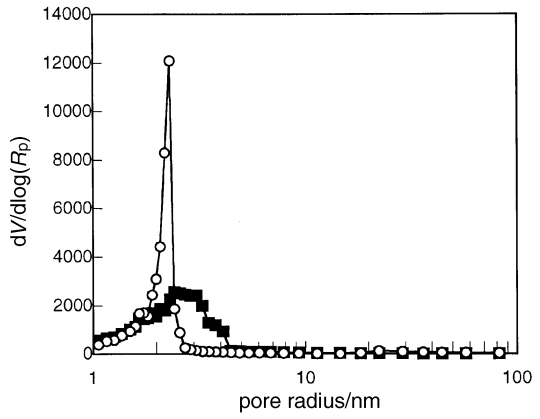

Fig. 7 Pore size distributions of the calcined (400 °C, 3 h) spheres estimated from the adsorption branch (●) and the desorption branch (○)

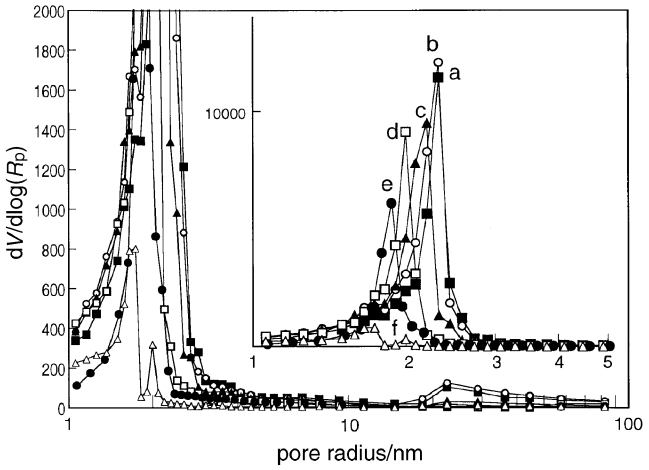

Fig. 8 Pore size distributions of the spheres at different calcination temperatures for 3 h. a, 200 °C (■); b, 400 °C (○); c, 600 °C (▲); d, 800 °C (□); e, 900 °C (●); f, 1000 °C (△). The smaller radius regions are shown in the inset.

than 100 nm could barely be detected by mercury porosimetry. On the other hand, the changing pore size distribution pattern with heat treatment was different from those of the silica xerogels reported so far,[29–31] in which the peak of the pore size distribution curve does not shift to smaller values when the calcination temperature increases. However, it was similar to those of ordered compacts of monosized silica spheres.[32] From the above results, it is considered that the spheres are composed of close-packed small spherical particles.

Table 2 shows the BET surface area, external surface area and pore volumes classified by the size range of the pores. The classified pore size ranges are generally called micropore (<2 nm), mesopore (2–50 nm) and macropore (>50 nm).[33] These classified pore volumes were evaluated by analysing the N_2 adsorption and desorption data according to the Dollimore–Heal method. S_{BET} of the gel calcined at 400 °C was the highest, 862 m^2 g^{-1}. Since the sample calcined at 200 °C still contained organic residues which could fill the pores, the S_{BET} value was lower than that of the sample calcined at 400 °C. Above 400 °C, the surface area decreased with increasing calcination temperature. The sample calcined at 1000 °C for 3 h still retained a surface area of 181 m^2 g^{-1}, though it was <1 m^2 g^{-1} after the calcination at 1100 °C. The external surface area (S_{ex}) came from the outer surface, which could be attributable to meso- and macro-pores, was very small compared to S_{BET}. This means that there exists a large portion of micropores. S_{ex} values of the samples calcined at different temperatures were only 2.8–4.5% of the whole BET surface areas. From V_P values the proportion of the pores could also be estimated. That is, the large part of the total pore volume of each gel calcined at different temperature is occupied by the pores whose diameters were less than 2 nm and between 2 and 10 nm. The proportion of the micropore volumes (<2 nm) to the volumes of the larger pores increased with increasing calcination temperature because of the shrinkage of the larger pores. The thermal change in total V_P was proportional to the change in surface area. Both values were decreased with increasing calcination temperature. The highest value, 1.008 ml g^{-1}, was obtained for the sample calcined at 400 °C. This means that after organics were removed at 300–400 °C the spheres were densified and shrank gradually with increasing calcination temperature.

As shown in the previous paragraph, the nitrogen adsorption isotherms exhibited sharp shoulders at low relative pressures and the BET surface area of the gel after the calcination at 400 °C was more than 800 m^2 g^{-1}. These facts suggest that the apparent primary particles as, seen in the SEM and TEM images, are not primary particles, which generally refer to highly dense particles. Assuming that the particles observed in Fig. 3c are compact (highly dense) particles of uniform size, the surface area should be proportional to the inverse of the particle diameter. The specific surface area of the gel composed of compact particles with 20 nm diameter, which is the typical size (SEM, TEM), is estimated to be only about 140 m^2 g^{-1} according to the geometrical calculation: $S=6/Dd$, where S is the surface area (in m^2 g^{-1}), D is the density of compact silica (2.2×10^6 g m^{-3}; the pycnometric densities of the spheres were ($2.1–2.2)\times10^6$ g m^{-3} in spite of the different calcination temperature) and d is the diameter of the elementary particles. Since the surface of the particle is not smooth, the surface area of the particle will be much higher. However, the gels prepared here are found to have very large surface areas for the size of the apparent primary particles. This means that even the 20 nm particles forming the gel have micropores smaller than 2 nm in diameter. As the calcination temperature increases, both micropores and mesopores shrink owing to densification of the skeleton structure. The smaller pores such as micropores, which contribute more to the surface area, shrink and disappear during calcination. This results in the steep decrease in surface area.

Table 2 S_{BET}, S_{ex} and V_p of the spherical silicas at various calcination temperatures

calcination temperature/°C	S_{BET}/m^2 g^{-1}	S_{ex}/m^2 g^{-1}	V_p				
			total/ml g^{-1}	<2 nm[a]/ml g^{-1}	2–10 nm/ml g^{-1}	10–50 nm/ml g^{-1}	>50 nm/ml g^{-1}
200	669	30	0.839	0.266	0.536	0.031	0.006
400	862	33	1.008	0.355	0.621	0.027	0.005
600	734	22	0.866	0.297	0.507	0.026	0.036
800	600	17	0.640	0.240	0.368	0.019	0.013
900	376	15	0.410	0.155	0.225	0.013	0.017
1000	181	6	0.134	0.072	0.056	0.005	0.001

[a]Pore diameter.

The spheres prepared here exhibit high surface areas and have small mesopores with diameters in the range 2–10 nm. These features are completely different from the spheres prepared by the so-called Stöber process, which are dense and show low porosity. In practice, the spheres in this study are formed in the emulsion while the Stöber particles arise in homogeneous solution. Since there are too many factors governing the formation of the spheres, it is difficult to explain the formation mechanism with a simple theory; however, it seems that the formation of the spheres occurs as illustrated in Fig. 5. This type of the apparent gelation was different from that in our previous report on the powder preparation,[19,20] in which the sol–gel process of TEOS with the organic acid starts from the homogeneous solution to produce a monolithic coagulum and then gives the mesoporous silica gel with a high surface area. However, the causes of the high surface area and mesopores will be same in both preparation processes. We consider that the acidity of tartaric acid and its hindrance effect towards the condensation of siloxane polymers causes such characteristics.[19,20]

Conclusion

Millimetre-sized mesoporous silica spheres were prepared directly from the reaction of tetraethoxysilane with tartaric acid in cyclohexanol by the sol–gel process. The scanning electron microscopy images showed that the spheres are basically composed of close-packed uniform small particles whose diameters are about 20 nm. The gels calcined at 400 °C showed specific surface areas of about 850 $m^2\ g^{-1}$ and gave sharp pore size (channel size) distribution curves spread in a narrow range around 2.3 nm radius. On the other hand, the cavity size was larger than the channel size but also spread in a narrow radius range between 1 and 4 nm. The peak of the pore size distribution curve shifted to smaller values as the calcination temperature increased from 400 to 900 °C, showing the same thermal behaviour as the ordered compacts of monosized silica spheres. The small particles forming the spheres were found to have micropores smaller than 2 nm in diameter, which contribute more to the surface area, by analysing the N_2 adsorption isotherm and the relationship between particle size and BET surface area. As a result, it was considered that the spheres are composed of close packing of the apparent primary particles which have large surface areas. On the other hand, the formation of the spheres or droplets will be basically same as the emulsion technique; however, the hydrolysis and condensation reaction of the droplets to form the spherical particles seem to occur from the surface of the droplets.

References

1 W. Stöber, A. Funk and E. Bohn, *J. Colloid Interface Sci.*, 1968, **26**, 62.
2 M. D. Sacks and T. Tseung-Yuen, *J. Am. Ceram. Soc.*, 1984, **67**, 526.
3 G. H. Bogush, M. A. Tracy and C. F. Zukoski IV, *J. Non-Cryst. Solids*, 1988, **104**, 95.
4 R. Masuda, W. Takahashi and M. Ishii, *J. Non-Cryst. Solids*, 1990, **121**, 389.
5 M. T. Harris, R. R. Brunson and C. H. Byers, *J. Non-Cryst. Solids*, 1990, **120**, 397.
6 A. van Blaaderen and A. P. M. Kentgens, *J. Non-Cryst. Solids*, 1992, **149**, 161.
7 E. C. Ruvolo Jr., H. L. Bellinetti and M. A. Aegerter, *J. Non-Cryst. Solids*, 1990, **121**, 244.
8 J. L. Woodhead, *Silicates Ind.*, 1972, **37**, 191.
9 Y. Nakahara, K. Motohashi, Y. Tanaka and K. Miyata, *J. Jpn. Soc. Color Mater.*, 1978, **51**, 521.
10 H. Yamauchi, H. Ishikawa and S. Kondo, *Colloids Surf.*, 1989, **37**, 71.
11 H. Yamashita, M. Demiya, H. Mori and T. Maekawa, *J. Ceram. Soc. Jpn.*, 1992, **100**, 1444.
12 Y. Moriya, N. Nishiguchi, M. Kawakami and R. Hino, *J. Ceram. Soc. Jpn.*, 1995, **103**, 570.
13 M. A. Butler, P. F. James and J. D. Jackson, *J. Mater. Sci.*, 1996, **31**, 1675.
14 M. Toba, F. Mizukami, S. Niwa, Y. Kiyozumi, K. Maeda, A. Annila and V. Komppa, *J. Mater. Chem.*, 1994, **4**, 585.
15 M. Toba, F. Mizukami, S. Niwa, T. Sano, K. Maeda, A. Annila and V. Komppa, *J. Mol. Catal.*, 1994, **91**, 277.
16 M. Toba, F. Mizukami, S. Niwa, T. Sano, K. Maeda and H. Shoji, *J. Mater. Chem.*, 1994, **4**, 1131.
17 K. Maeda, F. Mizukami, M. Watanabe, N. Arai, S. Niwa, M. Toba and K. Shimizu, *J. Mater. Sci. Lett.*, 1990, **9**, 511.
18 G. Zehl, S. Bischoff, F. Mizukami, H. Izutsu, M. Bartoszek, H. Jancke, B. Lucke and K. Maeda, *J. Mater. Chem.*, 1995, **5**, 1893.
19 H. Izutsu, F. Mizukami, Y. Kiyozumi and K. Maeda, *J. Am. Ceram. Soc.*, submitted.
20 H. Izutsu, F. Mizukami, T. Sashida, K. Maeda, Y. Kiyozumi and Y. Akiyama, *J. Non-Cryst. Solids*, in press.
21 D. Dollimore and G. R. Heal, *J. Appl. Chem.*, 1964, **14**, 109.
22 B. C. Lippens and J. H. De Bore, *J. Catal.*, 1965, **4**, 319.
23 G. W. Scherer, *J. Non-Cryst. Solids*, 1989, **109**, 183.
24 S. Brunauer, L. S. Deming, W. E. Deming and E. Teller, *J. Am. Chem. Soc.*, 1940, **62**, 1723.
25 S. J. Gregg and K. S. W. Sing, *Adsorption, Surface Area and Porosity*, Academic Press, London, 1982, p. 287.
26 K. Kaneko, *J. Membr. Sci.*, 1994, **96**, 59.
27 S. J. Gregg and K. S. W. Sing, *Adsorption, Surface Area and Porosity*, Academic Press, London, 1982, p. 129.
28 S. J. Gregg and K. S. W. Sing, *Adsorption, Surface Area and Porosity*, Academic Press, London, 1982, p. 151.
29 M. Yamane and S. Okano, *Yogyo-kyokai Shi*, 1979, **87**, 434.
30 A. M. Gadalla and S-J. Yun, *J. Non-Cryst. Solids*, 1992, **143**, 121.
31 R. K. Iler, *The Chemistry of Silica*, Wiley, New York, 1979, p. 545.
32 M. D. Sacks, T-Y. Tseng, *J. Am. Ceram. Soc.*, 1984, **67**, 532.
33 S. J. Gregg and K. S. W. Sing, *Adsorption, Surface Area and Porosity*, Academic Press, London, 1982, p. 25.

Paper 6/07333F; *Received* 28*th October*, 1996